

Analysis of a Parallel Solver for the Gray-Scott Reaction-Diffusion System

Parallel Programming for Large-Scale Problems SF2568
Teacher: Michael Hanke

Jonathan Ridenour, 780514-7779
Mateusz Herczka, 700624-9234

May 11, 2015

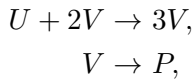
Problem description

The subject of this report is the parallelisation of a numerical method for a two-component reaction-diffusion system known as the Gray-Scott model. Originally introduced by Gray and Scott [1], the model is a system of two partial differential equations for the concentration of two chemical species, which are reacting with each other as they diffuse through a medium.

Pattern formation resulting from the Gray-Scott model is a rich area of research, with applications to a variety of physical, chemical, and biological phenomena, as well as cellular automata and the pattern formation of other partial differential equation systems [2]. We investigate a parallelisation strategy for the two-dimensional case. We make a series of trials, running the solver in parallel on 4, 16, 64, and 100 processes, and perform a speedup analysis using the results of these trials. Finally, we show a few of the various patterns that emerge from the Gray-Scott model with various input parameters.

Mathematical Formulation

The Gray-Scott model involves the reaction and diffusion of two generic chemical species, U and V , whose concentrations are described by the functions u and v , reacting according to the chemical equations



where P is an inert byproduct. This system is governed by the following system of partial differential equations, known as the Gray-Scott equations:

$$\frac{\partial u}{\partial t} = D_u \nabla^2 u - uv^2 + F(1-u), \quad u, v : \Omega \mapsto \mathbb{R}, \quad t \geq 0, \quad (1)$$

$$\frac{\partial v}{\partial t} = D_v \nabla^2 v + uv^2 - (F - K)v, \quad u, v : \Omega \mapsto \mathbb{R}, \quad t \geq 0. \quad (2)$$

Here, D_u and D_v are the diffusion constants for u and v respectively, and F and K are constants which govern the replenishment of the chemical species. The term uv^2 gives the reaction rate for the system. We are concerned with solving the Gray-Scott equations on a two-dimensional domain $\Omega = [0, 1]^2$. Thus, $u = u(x, y, t)$ and $v = v(x, y, t)$, giving the laplacian as

$$\begin{aligned} \nabla^2 u &= \frac{\partial^2 u}{\partial x^2} + \frac{\partial^2 u}{\partial y^2}, \\ \nabla^2 v &= \frac{\partial^2 v}{\partial x^2} + \frac{\partial^2 v}{\partial y^2}. \end{aligned}$$

As in [2], we use periodic boundary conditions for (1) and (2); thus, our simulation on Ω models a small surface surrounded by similar elements reacting identically. We

choose the diffusion constants $D_u = 2 \cdot 10^{-6}$, $D_v = 1 \cdot 10^{-6}$, and let F and K take values according to $F \in [0.02, 0.08]$, $K \in [0.05, 0.07]$ in order to investigate the different types of patterns that arise from varying combinations of the two.

The system is in a trivial state when $u = 1$ and $v = 0$. To initialize a reaction, we let the system assume this trivial state at time zero in all areas except a square in the middle of dimension one-sixth, where we set $u = 0.5$ and $v = 0.25$:

$$u(x, y, 0) = \begin{cases} 1/2, & 5/12 \geq x \geq 7/12, 5/12 \geq y \geq 7/12, \\ 1, & \text{otherwise,} \end{cases} \quad (3)$$

$$v(x, y, 0) = \begin{cases} 1/4, & 5/12 \geq x \geq 7/12, 5/12 \geq y \geq 7/12, \\ 0, & \text{otherwise.} \end{cases} \quad (4)$$

The reaction then diffuses outward from the middle, leaving behind a characteristic pattern, until all Ω is filled.

Numerical Method

We discretize Ω with the same stepsize in the x - and y -directions, h , corresponding to N^2 inner gridpoints equidistantly spread across the surface. We let $h = 1/(N + 1)$ such that $x_i = ih$, $i = 1, 2, \dots, N$ and $y_j = jh$, $j = 1, 2, \dots, N$. Thus the function value $u(x, y, t)$ is approximated by $u(ih, jh, t) = u_{i,j}(t)$, $t \geq 0$. Using the traditional central difference formula for the discrete five-point laplacian with step length h , Δ_5^h , the system (1) + (2) can be written in semi-discrete form as follows:

$$\frac{\partial u_{i,j}}{\partial t} = \frac{D_u}{h^2} \Delta_5^h u_{i,j} - u_{i,j}(v_{i,j})^2 + F(1 - u_{i,j}), \quad (5)$$

$$\frac{\partial v_{i,j}}{\partial t} = \frac{D_v}{h^2} \Delta_5^h v_{i,j} + u_{i,j}(v_{i,j})^2 - (F - K)v_{i,j}. \quad (6)$$

We then discretize in time, with timestep dt , and approximate the time-derivative with the explicit Euler method. Letting $t = k \cdot dt$ for $k = 1, 2, 3, \dots$, and $u_{i,j}(k \cdot dt) = u_{i,j}^k$, $v_{i,j}(k \cdot dt) = v_{i,j}^k$, the system (5) + (6) becomes

$$\frac{u_{i,j}^{k+1} - u_{i,j}^k}{dt} = \frac{D_u}{h^2} \Delta_5^h u_{i,j}^k - u_{i,j}^k(v_{i,j}^k)^2 + F(1 - u_{i,j}^k), \quad (7)$$

$$\frac{v_{i,j}^{k+1} - v_{i,j}^k}{dt} = \frac{D_v}{h^2} \Delta_5^h v_{i,j}^k + u_{i,j}^k(v_{i,j}^k)^2 - (F - K)v_{i,j}^k. \quad (8)$$

The difference equations (7) and (8) give a simple formula for the update of the function values at time $(k + 1) \cdot dt$ given that values at time $k \cdot dt$. We represent the discrete functions $u_{i,j}^k$ and $v_{i,j}^k$ as long vectors \mathbf{u}^k and \mathbf{v}^k with the following enumeration:

$$\begin{aligned} \mathbf{u}^k &= (u_{1,1}^k, u_{2,1}^k, \dots, u_{N,1}^k, u_{1,2}^k, u_{2,2}^k, \dots, u_{N,N}^k), \\ \mathbf{v}^k &= (v_{1,1}^k, v_{2,1}^k, \dots, v_{N,1}^k, v_{1,2}^k, v_{2,2}^k, \dots, v_{N,N}^k). \end{aligned}$$

Using the long vectors, we can write the numerical operator Δ_5^h as a sparse matrix multiplication as follows:

$$\frac{D_u}{h^2} \Delta_5^h u_{i,j} = \mathbf{A}_u \mathbf{u}^n,$$

$$\frac{D_v}{h^2} \Delta_5^h v_{i,j} = \mathbf{A}_v \mathbf{v}^n,$$

where the matrices \mathbf{A}_u and \mathbf{A}_v are of dimension $[N^2 \times N^2]$ with block tridiagonal form:

$$\begin{aligned}\mathbf{A}_u &= \text{tridiag}_N(\sigma_u \mathbf{I}, \mathbf{T}_u, \sigma_u \mathbf{I}), \\ \mathbf{A}_v &= \text{tridiag}_N(\sigma_v \mathbf{I}, \mathbf{T}_v, \sigma_v \mathbf{I}),\end{aligned}$$

where \mathbf{I} is an identity matrix, multiplied by the constants σ_u or σ_v , and the matrices \mathbf{T}_u and \mathbf{T}_v are tridiagonal of the form

$$\begin{aligned}\mathbf{T}_u &= \text{tridiag}_N(\sigma_u, -4\sigma_u, \sigma_u), \\ \mathbf{T}_v &= \text{tridiag}_N(\sigma_v, -4\sigma_v, \sigma_v),\end{aligned}$$

where

$$\sigma_u = \frac{D_u}{h^2},$$

$$\sigma_v = \frac{D_v}{h^2}.$$

If we let $f_u(\mathbf{u}^k, \mathbf{v}^k) = -\mathbf{u}^k(\mathbf{v}^k)^2 + F(1 - \mathbf{u}^k)$ and $f_v(\mathbf{u}^k, \mathbf{v}^k) = \mathbf{u}^k(\mathbf{v}^k)^2 - (F - k)\mathbf{v}^k$, we can compactly write the fully discretized equations as

$$\mathbf{u}^{k+1} = \mathbf{u}^k + dt[\mathbf{A}_u \mathbf{u}^k + f_u(\mathbf{u}^k, \mathbf{v}^k)], \quad (9)$$

$$\mathbf{v}^{k+1} = \mathbf{v}^k + dt[\mathbf{A}_v \mathbf{v}^k + f_v(\mathbf{u}^k, \mathbf{v}^k)], \quad (10)$$

and we have an exact update formula for each time step.

Initial and Boundary Conditions

The initial and boundary conditions are straightforward to implement numerically. The initial state is completely known, so \mathbf{u}^0 and \mathbf{v}^0 are given. To implement periodic boundary conditions we simply set

$$\begin{aligned}u_{-1,j}^k &= u_{N-1,j}^k, \\ u_{i,-1}^k &= u_{i,N-1}^k, \\ u_{N,j}^k &= u_{0,j}^k, \\ u_{i,N}^k &= u_{i,0}^k,\end{aligned}$$

when updating the boundary points. The formula is likewise for v .

Stability Conditions

In order to ensure numerical stability for the differential operators \mathbf{A}_u and \mathbf{A}_v in (9) and (10), we must conform to the restriction

$$dt \cdot \lambda_{l,u} \in \mathcal{S}, \forall l, l = 1, 2, \dots, L_u,$$

$$dt \cdot \lambda_{l,v} \in \mathcal{S}, \forall l, l = 1, 2, \dots, L_v,$$

where $\lambda_{l,u}$ and $\lambda_{l,v}$ are the l -th eigenvalues of \mathbf{A}_u and \mathbf{A}_v respectively, and \mathcal{S} is the stability region of the explicit Euler method: a circle in the complex plane centered at -1 with unit radius [3]. The number of unique eigenvalues possessed by each of the matrices is denoted by L_u and L_v .

For the parallel speedup trials, we discretize Ω using $N = 400$. Together with the chosen diffusion constants, the maximum eigenvalue, λ_{max} , of \mathbf{A}_u and \mathbf{A}_v has a strictly negative real value, and thus we must choose a timestep such that $dt \cdot \lambda_{max}$ is at least -2 . The maximum eigenvalue is computed using Matlab as:

$$\lambda_{max} = -1.2735,$$

which provides the limitation on the timestep:

$$dt \leq \frac{-2}{-1.2735} = 1.5704.$$

Since the timestep also has a damping effect on the replenishment term and reaction rate, we must consider these as well when choosing the timestep. As in [2], we settle on a value which is comfortably beneath the max:

$$dt = 0.75.$$

This is well within the stability bounds imposed by \mathbf{A}_u and \mathbf{A}_v ; it also provides suitable damping on the replenishment and reaction rate terms for the observation of the characteristic Gray-Scott pattern formation.

Algorithm Description

Implementation details

To implement the update formulae (9) and (10) in parallel, the computational domain is divided into subdomains, one for each process. Each process is responsible for the update of its local values. Along the subdomain boundaries, neighbouring values are needed for the update; these are obtained by coordinated message-passing. The boundary data are communicated between processes by means of a red-black communication schedule. When all necessary information is obtained, the local values are updated according to (9) and (10), see Algorithm 5.

For a domain size of 400×400 , the global update boils down to two matrix multiplications, one using \mathbf{A}_u , one using \mathbf{A}_v , each of which contains 400^4 elements, most of

which are zero. This can be accomplished by means of a sparse matrix multiplication method, or direct kernel computations. First we describe their common structure.

The 5-point computation molecule is dependent on four neighbours labeled NORTH, EAST, SOUTH and WEST. We define a 2D cartesian mesh of p^*p processes, where $p = \sqrt{P}$. The N^*N domain is decomposed into P square subdomains, each with dimension $n*n$ elements, where $n = \sqrt{N}$. The challenge becomes to communicate the domain borders between neighbours, and synchronize this with computation of the domain interior. Our red-black scheme is shown in Algorithm 1.

```

if (even row AND even process) OR (odd row AND odd process) then
    |   color := red;
else
    |   /* (even row AND odd process) OR (odd row AND even process) */ 
    |   color := black;
end
```

Algorithm 1: Determining process color

The 2D process grid is thus colored in a checkerboard pattern. Since we use periodic boundary conditions, we assume even p to ensure red-black neighbours when wrapping around the boundaries of the grid. Because the subdomain borders are shared between neighbours, we implement overlap by introducing a ghost frame surrounding the subdomain, labeled GHOST_NORTH, GHOST_EAST, GHOST_SOUTH and GHOST_WEST, which give each subdomain a total dimension of $(n+2)*(n+2)$. In addition, we define four borders of the inner $n \times n$ domain, labeled BORDER_NORTH, BORDER_EAST etc. The values in the borders are recalculated every iteration, then sent to the corresponding neighbour. The values in the ghosts are used when the computation molecule centers on an element at a border. They are received from a neighbour every iteration before the computation phase starts.

Algorithm 2 shows how each computation is preceded by a communication phase arranged in four parts to avoid deadlock. Each sendreceive is done once for u and once for v . We also show the timing calls.

```

while iter < maxiter do
    start := startTimer();
    if (red) then
        /* paramlist (sendbuffer, receivebuffer, neighbour) */
        sendreceive(BORDER_NORTH, GHOST_NORTH, neighbour[NORTH]);
        sendreceive(BORDER_SOUTH, GHOST_SOUTH, neighbour[SOUTH]);
        sendreceive(BORDER_EAST, GHOST_EAST, neighbour[EAST]);
        sendreceive(BORDER_WEST, GHOST_WEST, neighbour[WEST]);
    else
        /* black */
        sendreceive(BORDER_SOUTH, GHOST_SOUTH, neighbour[SOUTH]);
        sendreceive(BORDER_NORTH, GHOST_NORTH, neighbour[NORTH]);
        sendreceive(BORDER_WEST, GHOST_WEST, neighbour[WEST]);
        sendreceive(BORDER_EAST, GHOST_EAST, neighbour[EAST]);
    end
    end := endTimer();
    tComm += end-start;
    start := startTimer();
    calculateDomain();
    end := endTimer();
    tCalc += end-start;
    iter++;
end

```

Algorithm 2: Sendreceive phases with timing calls

We now describe the specifics our two implementations, which differ mainly in the calculateDomain() procedure. The matrix version uses a small sparse matrix library called CSparse, authored by Timothy Davis, who has contributed to several matrix routines in MATLAB as well as NVIDIA [4]. While fast, it's not fully competitive with professional libraries. Yet the code is readable and enables us to formulate code similar to MATLAB and formulas (9) and (10). CSparse doesn't reference any other libraries, so the code is portable between our laptops and Ferlin. Algorithm 3 shows the expressions for u, with v being analogous.

```

foreach element i in u do
    unew[i] = u[i] + ht * ( (-u[i] * v[i]2) + (F * (1.0 - u[i])) )
    /* CSparse call equivalent to:  unew = Au*v + unew, */ 
    /* where Au is a constant, sparse matrix. */ 
    csGaxpy(Au, u, unew);
    unew[boundaries] += sigma * ghost;
end

```

Algorithm 3: Sparse matrix implementation of calculateDomain()

Algorithm 4 shows how the kernel version computes the 5-point molecule for each domain element with a direct expression.

```

ru = (ht * DU)/(hx)2;
foreach element i in u do
    unew[i][j] = u[i][j] + ru * (u[i - 1][j] - (4 * u[i][j]) +
        u[i + 1][j] + u[i][j - 1] + u[i][j + 1]) +
        ht * (-u[i][j] * v[i][j] * v[i][j] + F * (1.0 - u[i][j])); 
end

```

Algorithm 4: Kernel implementation of calculateDomain()

The east and west borders/ghosts are columns and thus non-contiguous in memory. The matrix implementation maintains two work buffers for this data, which is arranged sequentially and copied into these buffers before IO, which results in extra work due to the copy operations. In the kernel implementation we instead define an MPI_Type_vector which omits the buffer copying. MPI_Cart functions are used to set up an mpi process mesh. This allows for defining arrays of neighbour coordinates, including diagonals for future use with a 9-point kernel, and is also easy to extend into 3D.

Finally, our programs save the domains as matrix blocks which are automatically assembled and plotted in MATLAB.

```

Data:  $dt, \mathbf{u}^k, \mathbf{v}^k, \mathbf{A}_u, \mathbf{A}_v, red$ 
Result:  $\mathbf{u}^{k+1}$  and  $\mathbf{v}^{k+1}$ 
collect boundary data  $\mathbf{b}_{out}$ ;
if  $red$  then
| send  $\mathbf{b}_{out}$ : north, south, east, west;
| receive  $\mathbf{b}_{in}$ : south, north, west, east;
else
| receive  $\mathbf{b}_{in}$ : south, north, west, east;
| send  $\mathbf{b}_{out}$ : north, south, east, west;
end
 $\mathbf{u}^{k+1} = \mathbf{u}^k + dt[\mathbf{A}_u \mathbf{u}^k + f_u(\mathbf{u}^k, \mathbf{v}^k)] + \mathbf{b}_{in};$ 
 $\mathbf{v}^{k+1} = \mathbf{v}^k + dt[\mathbf{A}_v \mathbf{v}^k + f_v(\mathbf{u}^k, \mathbf{v}^k)] + \mathbf{b}_{in};$ 

```

Algorithm 5: Communication and local update.

Performance Evaluation

Extrapolated Speedup

In an attempt to predict the parallel speedup we can expect to achieve as we increase the number of processes, we perform an initial run on 1 and 4 processes, compute the speedup S_4 , and extrapolate to S_P using Amdahl's Law. For the test case employing sparse matrix multiplication, we get an run time of 793.15 s on one process, and 304.39 s on 4 processes. This gives the initial speedup:

$$S_4 = \frac{T_1}{T_4} = 2.606.$$

Using Amdahl's Law we can solve for f , the fraction of the computation which cannot be divided into parallel tasks:

$$S_4 = \frac{4}{1 + 3f} \Rightarrow f = \frac{4 - S_4}{3S_4} = 0.1783.$$

Applying this same analysis to the kernel method, we get the following calculation:

$$S_4 = \frac{T_1}{T_4} = \frac{113.0}{94.26} = 1.199 \Rightarrow f = \frac{4 - S_4}{3S_4} = 0.7789.$$

Table 1 shows the extrapolated speedup that these values for f indicate for 16, 64, and 100 processes. This method is obviously a poor predictor for both the parallelisation strategies we employ. Indeed, our experimental speedup trials indicate that the problem scales very well on increased numbers of processes, see figures 1 and 2.

Table 1: Extrapolated speedup given by Amdahl's Law.

	P	4	16	64	100
Sparse matrix method	S_P	2.6	4.3	5.2	5.4
Kernal method	S_P	1.2	1.3	1.3	1.3

Experimental Speedup

We run a series of trials on Ferlin and record the initialisation time, t_{init} , the communication time, t_{comm} , the calculation time, t_{calc} , and the total run time t_{tot} . Tables 4 and 3 show the maximum of these values for each of the trials at 1, 4, 16, 64, and 100 processes. The values of t_{tot} are used to compute the experimental speedup, shown in figures 1 and 2.

Table 2: Max time (seconds) measurements, sparse matrix method.

P	t_{init}	t_{comm}	t_{calc}	t_{tot}
1	0.1437	0.000	793.0	703.14
4	0.05663	36.48	301.8	304.4
16	0.008907	8.786	38.42	40.87
64	0.009324	2.8460	7.391	9.603
100	0.001253	3.206	4.287	7.419

Table 3: Max time (seconds) measurements, kernel method.

P	t_{init}	t_{comm}	t_{calc}	t_{tot}
1	0.0046	0.0000	113.0	113.0
4	0.0051	3.157	91.37	94.26
16	0.1540	3.115	6.559	9.778
64	0.1845	2.410	1.683	4.248
100	1.197	3.293	1.081	5.556

Larger Domain

Using the faster kernel method, we conduct another numerical experiment on Ferlin with a 1000x1000 domain and same number of iterations. We find that $dt = 0.075$ is sufficient

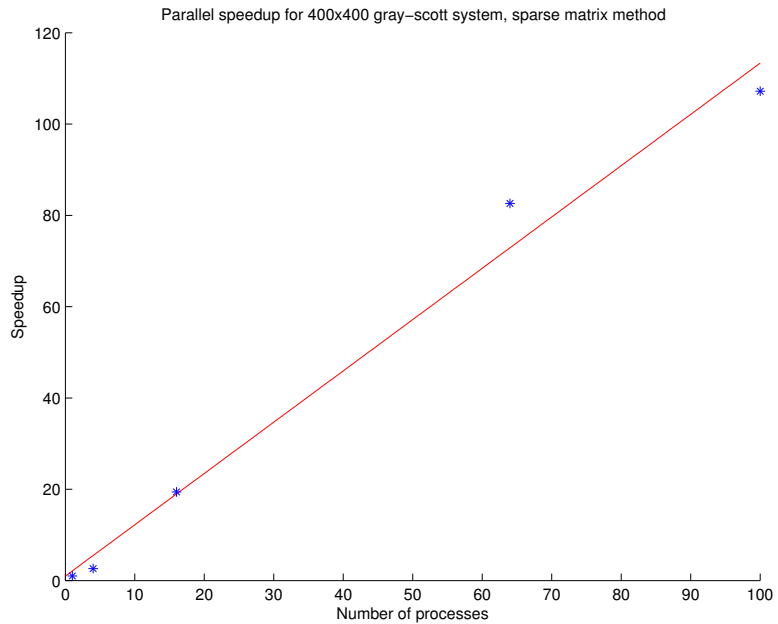


Figure 1: Experimental speedup, sparse matrix multiplication method.

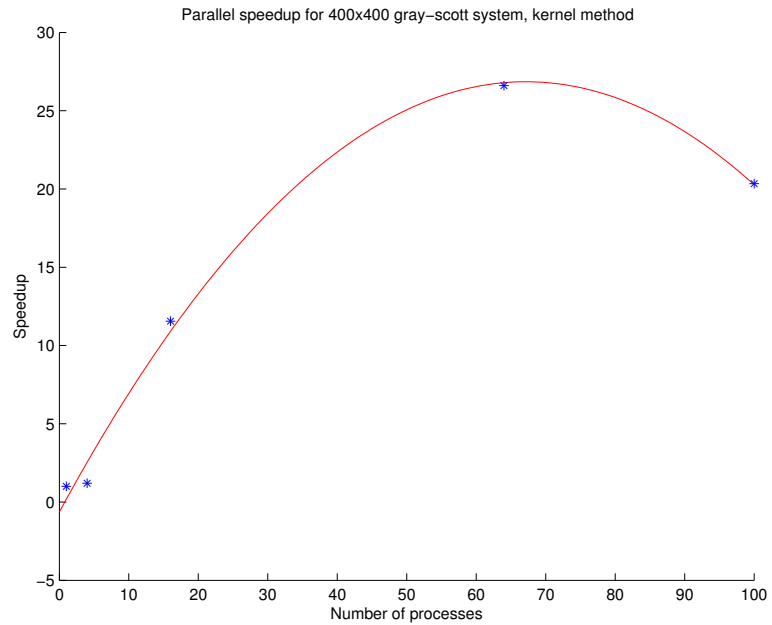


Figure 2: Experimental speedup, kernel method.

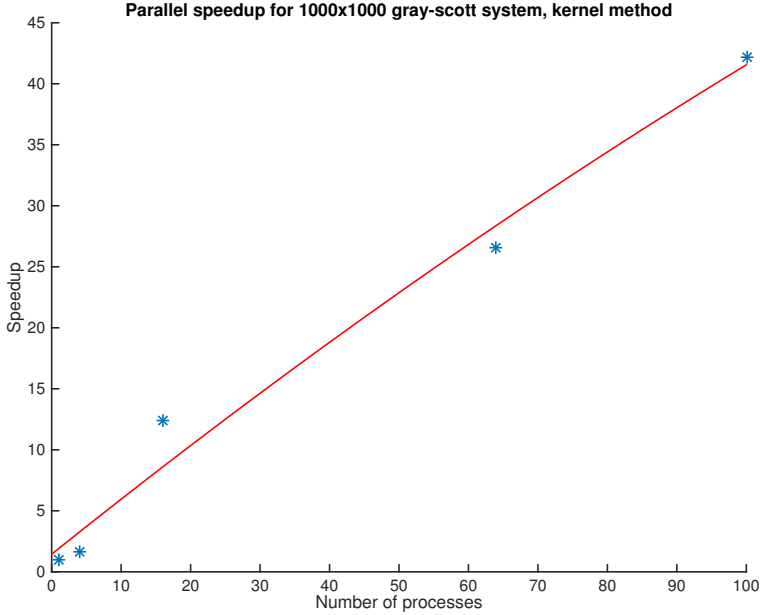


Figure 3: Experimental speedup, kernel method, 1000x1000 domain.

for stability, while still yielding a pattern growth which almost fills the entire domain. As before, we run 1, 4, 16, 64, and 100 processes.

Table 4: Max time (seconds) measurements, kernel method, 1000x1000 domain.

P	t_{init}	t_{comm}	t_{calc}	t_{tot}
1	0.02936	0.000	756.86	756.89
4	0.00555	71.502	398.283	469.79
16	0.06474	14.1897	47.0218	61.276
64	0.1676	11.099	17.286	28.553
100	1.1956	10.215	6.5125	17.923

Speedup Analysis

There are a few reasons why the extrapolation of Amdahl's Law does not provide an accurate predictor for the parallel speedup. The most obvious reason is that f , the fraction of the computation which cannot be divided into parallel tasks, does not in itself account for an upper bound on the speedup. In fact, our best measure of f is t_{init} and, as can be seen in tables 4 and 3, this accounts for only a minuscule portion of the total

runtime. It is more likely that the speedup can be explained by the memory hierarchies employed by Ferlin.

** TVEKSAMT vi vet inget om hur ferlin är byggd. When the number of processes is low, so is the available cache. As the number of processes increases, more of the working set, and at some point the entire working set, can fit into the available caches, allowing for a quicker memory access time. **

The matrix implementation shows a slightly supralinear speedup with a final efficiency of ≈ 1.1 at 100 processes. The good speedup is likely to come from the fact that the implementation is slow to begin with.

On the other hand, the kernel implementation (which is several times faster both sequentially and in parallel), accesses memory in a linear fashion more favorable for caching. The faster kernel implementation shows a sharp drop in speedup after 64 processes, the final efficiency being ≈ 0.22 . For the kernel with larger domain, final efficiency ≈ 0.42 with a more linear curve.

IN order to investigate the fraction between computation and other efforts, we calculate $(t_{init} + t_{comm})/t_{calc}$ at $P = 100$ yields 0.75 for matrix, 4.15 for kernel and 2.76 for kernel with larger domain. Clearly the calculation effort is dominated by communication and initialization as the problem size per process decreases.

Cache architecture surely effects performance as well, considering that the implementations don't access memory in the same order. We conclude that there exists an optimal problem size per process. If too small, it will fail to exploit the system architecture and fully utilize the processor power. For a sufficiently large problem, the kernel implementation shows sublinear but constant speedup.

Patterns

A variety of patterns

Conclusions

Both our algorithms scale well with problem size and increasing P , as long as care is taken to sufficiently load each processor. The kernel implementation is consistently the faster method despite the poorer speedup. Profiling is essential for the problem at hand, on the system which will perform the computations, in order to optimize problem size per process.

Finally, the explicit method may not be optimal if implicit methods can be found which speed up convergence sufficiently to counteract expensive global operations.

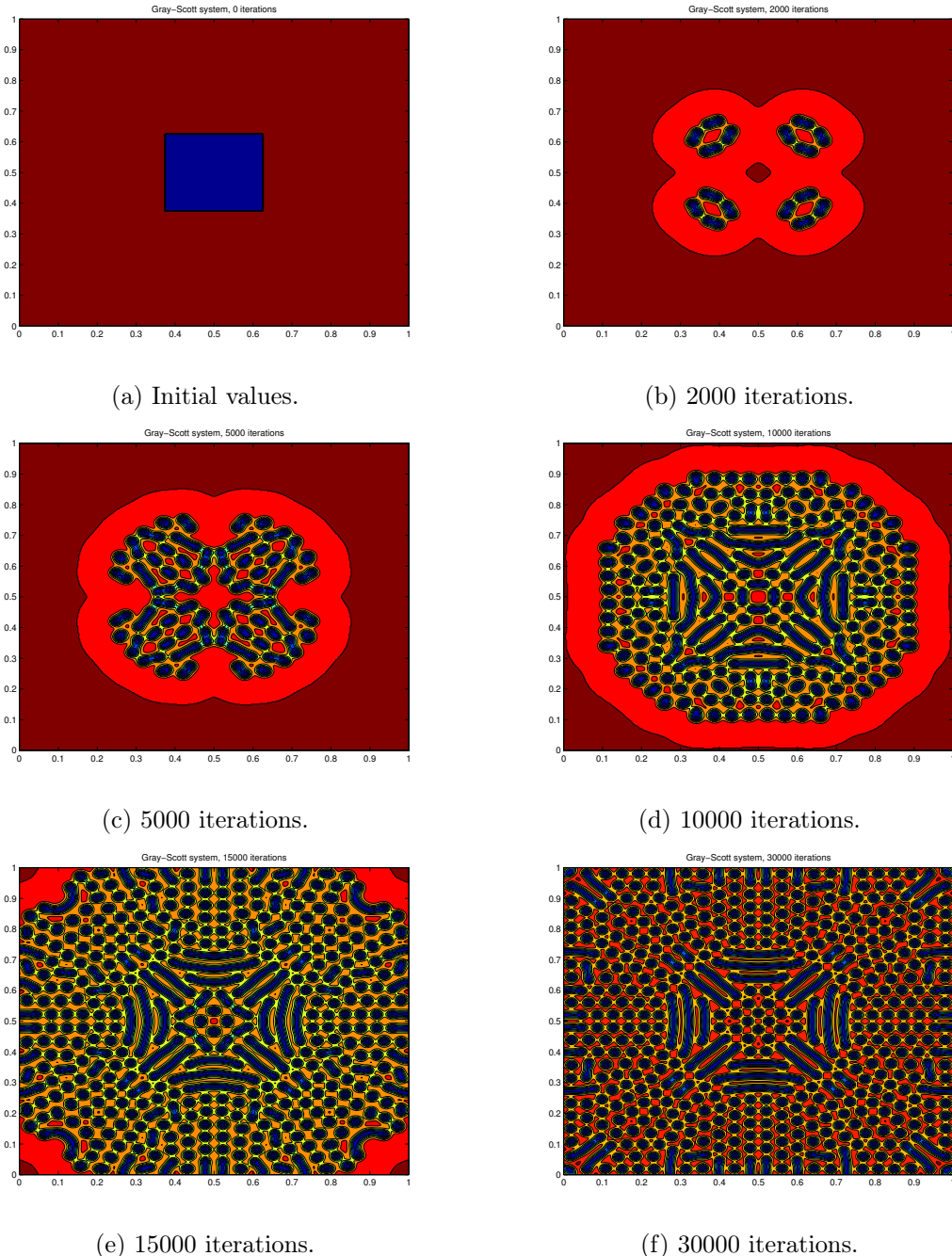


Figure 4: Reaction and diffusion of the Gray-Scott system, $F = 0.0375$, $K = 0.0634$.

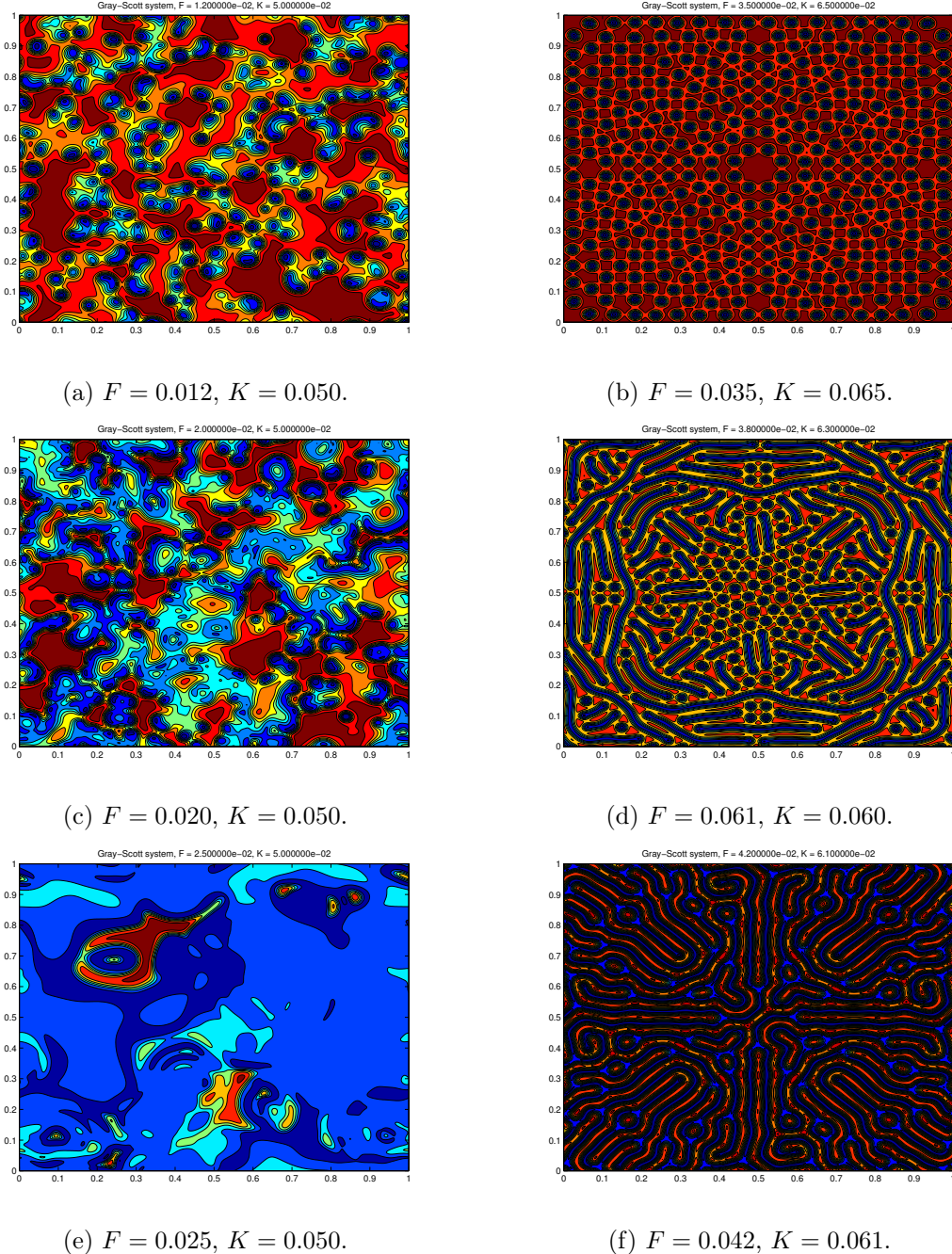


Figure 5: The Gray-Scott system, 50000 iterations for various F and K .

References

- [1] Gray P, Scott SK. *Sustained oscillations and other exotic patterns of behavior in isothermal reactions*. J Phys Chem 1985;89:22–32.
- [2] Weiming Wang, Yezhi Lin, Feng Yang, Lei Zhang, Yongji Tan, *Numerical study of pattern formation in an extended Gray–Scott model*, Communications in Nonlinear Science and Numerical Simulation, 16 (2011).
- [3] Lennart Edsberg *Introduction to Computation and Modelling for Differential Equations*, 2008, John Wiley and Sons, pp 50.
- [4] Timothy Davis, *Direct Methods for Sparse Linear Systems*, Society of Industrial and Applied Mathematics, 2006.